

## Cathode properties of layered structure $\text{Li}_2\text{PtO}_3$

Kaoru Asakura<sup>a,\*</sup>, Shigeto Okada<sup>b</sup>, Hajime Arai<sup>a</sup>, Shin-ichi Tobishima<sup>a</sup>, Yoji Sakurai<sup>a</sup>

<sup>a</sup> NTT Integrated Information and Energy Systems Laboratories, Tokai-mura, Ibaraki-ken, 319-1193, Japan

<sup>b</sup> Institute of Advanced Material Study, Kyushu University, Kasuga-shi, Fukuoka-ken, 816-8580, Japan

### Abstract

$\text{Li}_2\text{MO}_3$  (M: transition metal), which has a similar layer structure to  $\text{LiCoO}_2$ , is interesting for use as another layered rocksalt-type oxide cathode for Li-ion batteries. We found that  $\text{Li}_2\text{PtO}_3$  in  $\text{Li}_2\text{MO}_3$  system is the first full 4 V class cathode material among 5d metal compounds. We investigated the electrochemical, structural and kinetic characteristics of the 4 V region. The volumetric capacity of the 4 V plateau on discharge is comparable to that of  $\text{LiCoO}_2$ . Moreover, the reversibility of the structural change in the 4 V region was confirmed by X-ray diffractometry. © 1999 Elsevier Science S.A. All rights reserved.

**Keywords:** Lithium-ion cell; Intercalation; Layered rocksalt; Cathode

### 1. Introduction

Of the rocksalt-type ternary oxides,  $\text{LiCoO}_2$  and  $\text{LiNiO}_2$  with an  $\alpha\text{-NaFeO}_2$  [1] type structure have been most intensively studied for use as 4 V cathode materials in practical Li ion batteries. They have a layered rocksalt superstructure with alternate cationic (111) planes of Li and M which occupy the octahedral sites of a cubic close packing of oxygens. The two dimensional Li diffusion paths between the oxygen layers allow the reversible electrochemical extraction of lithium with fast electrode kinetics.

Other layered rocksalt-related oxides  $\text{Li}_2\text{MO}_3$  also have the similar structure to  $\alpha\text{-NaFeO}_2$  as shown in Fig. 1 and could be expected to have similar electrode kinetics to  $\text{LiCoO}_2$  and  $\text{LiNiO}_2$ . All  $\text{Li}_2\text{MO}_3$  compounds reported so far, except  $\text{Li}_2\text{ZrO}_3$  can be represented as  $(\text{Li}^+)_{3a}(\text{Li}_{1/3}^+\text{M}_{2/3}^{4+})_{3b}\text{O}_2$  [2]. Of these potential cathode materials, most attention has been directed to  $\text{Li}_2\text{MO}_3$  with Mo [3], Ru [4], Ir [5], Mn [6] and Pt [7] as M. Because the pentavalent or hexavalent state of M retains the charge neutrality and the layer structure at a fully charged state,  $\text{Li}_{2-x}\text{M}^{+(4+x)}\text{O}_3$ . In fact, they can all with the exception of  $\text{Li}_2\text{MnO}_3$ , reversibly deintercalate Li from the initial composition.

This paper describes the electrochemical, structural and kinetic characteristics of  $\text{Li}_2\text{PtO}_3$  and introduces  $\text{Li}_2\text{PtO}_3$

as the first 4 V cathode material providing 100 mA h/g from among the 5d transition metal compounds.

### 2. Experimental

$\text{Li}_2\text{PtO}_3$  was prepared by firing a 1:1 molar ratio mixture of reagent grade lithium carbonate (Kanto Chemical, 99%) and platinum black (Furuuchi Chemical, 99.98%) at 800°C for 1 day in air. Products thus obtained were identified by X-ray powder diffractometry (XRD, Rigaku Rotaflex) with monochromated  $\text{CuK}\alpha$  radiation.

The electrochemical cathode performance was evaluated in coin-type lithium cells (23 mm in diameter and 2 mm thick). The  $\text{Li}_2\text{PtO}_3$  working electrode was fabricated by mixing the obtained  $\text{Li}_2\text{PtO}_3$  powder, acetylene black (Denki Kagaku) and PTFE Teflon binder (Daikin) in a weight ratio of 70:25:5, respectively. The electrolyte was a solution of 1 M  $\text{LiPF}_6$  dissolved in a 50/25/25 vol.% (v/o) mixture of 1,2-dimethyl carbonate (DMC), propylene carbonate (PC) and ethylene carbonate (EC), respectively. This electrolyte has often been used for high voltage cathodes, because of its resistance to oxidation [8]. The cells were galvanostatically cycled between voltage limits of 3.5 and 4.5 V at a current density of 0.5 mA/cm<sup>2</sup> using a computer-controlled cycler system.

Structural changes in the cathode during the charge/discharge cycle were measured by XRD. After reaching potential equilibrium, each cathode pellet was adequately rinsed with dimethyl carbonate and dried in vacuum.

\* Corresponding author

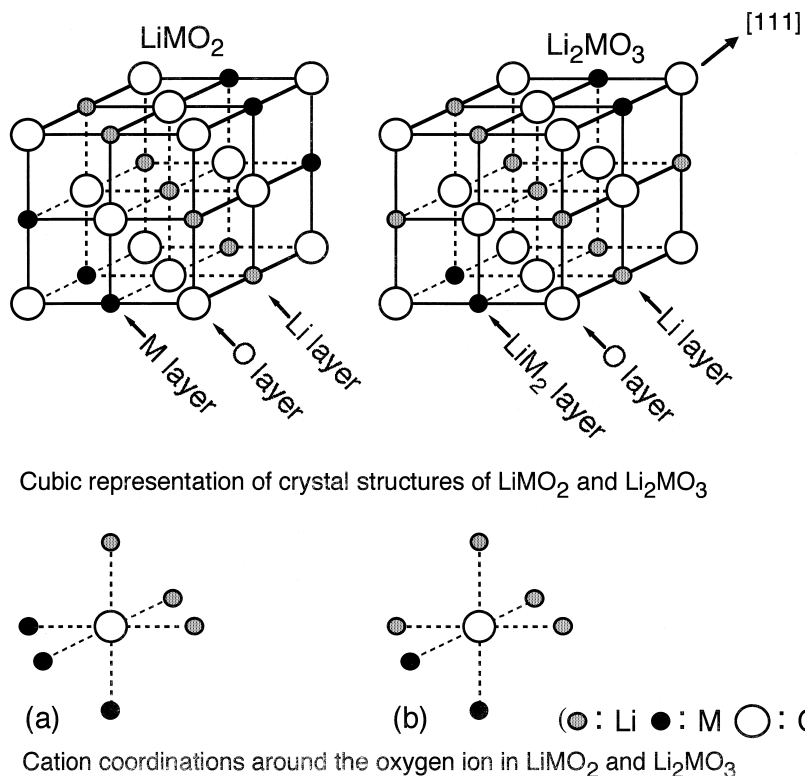


Fig. 1. Cubic representation of  $\text{LiMO}_2$  and  $\text{Li}_2\text{MO}_3$  layered rocksalt structure. (a) is the only possible coordination of the oxygen atoms in layered rocksalt  $\text{LiMO}_2$  and only the configuration in (b) is geometrically possible for layered rocksalt  $\text{Li}_2\text{MO}_3$  except  $\text{Li}_2\text{ZrO}_3$ .

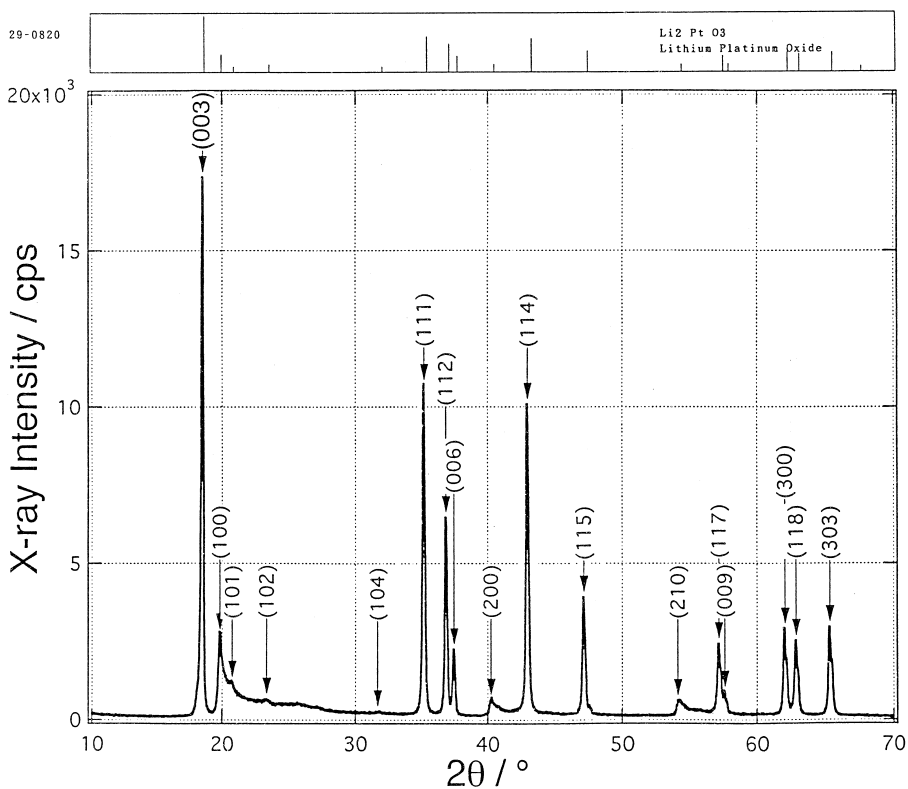


Fig. 2. XRD profile of  $\text{Li}_2\text{PtO}_3$  with  $\text{CuK}\alpha$  radiation.

### 3. Results and discussion

#### 3.1. Identification of $\text{Li}_2\text{PtO}_3$

The X-ray diffraction patterns of the yellow  $\text{Li}_2\text{PtO}_3$  powders we obtained could be indexed to a hexagonal unit cell ( $\text{P3}_1$ ;  $a = 5.17 \text{ \AA}$ ,  $c = 14.42 \text{ \AA}$ ) as shown in Fig. 2. All the peaks match those given for  $\text{Li}_2\text{PtO}_3$  in the JCPDS powder diffraction card No. 29-0820 well with no extra peaks.

#### 3.2. Electrochemical properties of $\text{Li}_2\text{PtO}_3$

The charge/discharge curve of  $\text{Li}_{2-x}\text{PtO}_3$  is shown in Fig. 3 with the congener. The lithium ions can be removed up to  $x = 1.2$  from  $\text{Li}_{2-x}\text{PtO}_3$  by charging to 4.5 V. The discharge curve after oxidative lithium extraction exhibits a 4 V region, which is very similar to that of  $\text{LiCoO}_2$  and  $\text{LiNiO}_2$ .  $\text{Li}_2\text{PtO}_3$  have a relatively large irreversible capacity at the 1st cycle in the same manner as  $\text{Li}_2\text{IrO}_3$  and  $\text{Li}_2\text{RuO}_3$ . However, after the 1st cycle, the charge and discharge curves are very similar to each other and the polarization ( $V_{\text{charge}} - V_{\text{discharge}}$ ) is less than 0.5 V at a rate of  $0.5 \text{ mA/cm}^2$ . The rechargeable capacity in the 4 V region is about  $100 \text{ mA h/g}$ . Although the gravimetric capacity is smaller than that of  $\text{LiCoO}_2$ , as shown in Fig. 4, the volumetric capacity ( $764 \text{ mA h/cm}^3$ ) exceeded that of  $\text{LiCoO}_2$ , because the density of  $\text{Li}_2\text{PtO}_3$  is 1.5 times that of  $\text{LiCoO}_2$ .

The rechargeability of the 4 V region was electrochemically confirmed in various voltage ranges in the  $\text{Li}/\text{Li}_{2-x}\text{PtO}_3$  cell as shown in Fig. 5. After charging to 5.0 V, the 4 V region disappeared in the discharge curve. This undoubtedly caused by cathode degradation or electrolyte oxidation breakdown. However, there seem to be no serious problems in the cell on charging to 4.6 V. Between 3.5 and 4.5 V, the specific capacity of the 4 V

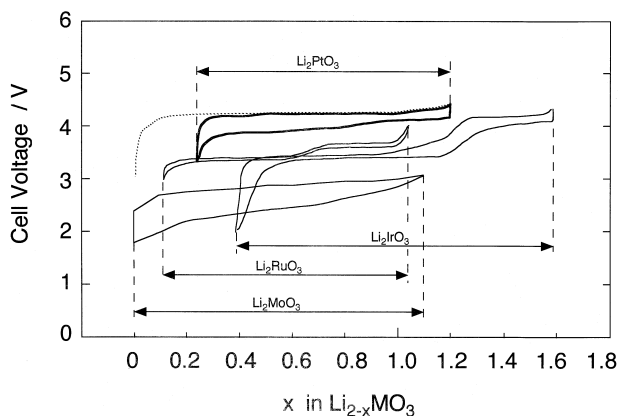


Fig. 3. Charge–discharge profiles of several  $\text{Li}_{2-x}\text{MO}_3$  cathodes. The  $\text{Li}/\text{Li}_2\text{PtO}_3$  cell was cycled at a rate of  $0.5 \text{ mA/cm}^2$  between 3.5 V and 4.5 V;  $\text{Li}_2\text{PtO}_3$ :  $100 \text{ mA h/g}$ ,  $\text{Li}_2\text{IrO}_3$ :  $130 \text{ mA h/g}$  [5],  $\text{Li}_2\text{RuO}_3$ :  $160 \text{ mA h/g}$  [4],  $\text{Li}_2\text{MoO}_3$ :  $180 \text{ mA h/g}$  [3]. Dotted line shows first charge.

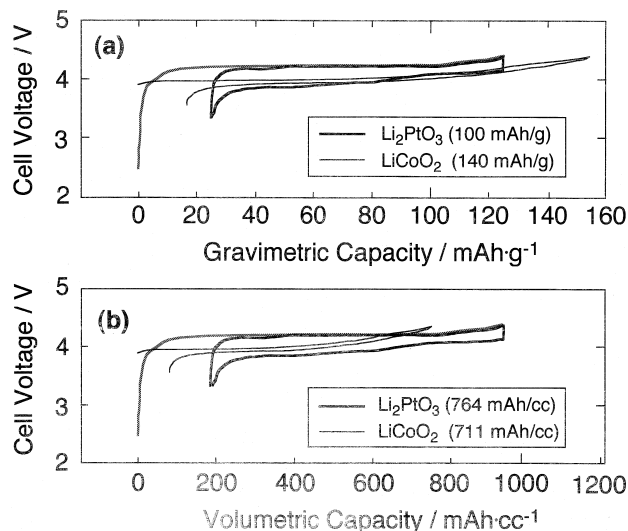


Fig. 4. Specific capacities of  $\text{Li}/\text{LiCoO}_2$  and  $\text{Li}/\text{Li}_2\text{PtO}_3$  cell; comparison of (a) gravimetric capacity, and (b) volumetric capacity.

region slowly decreases and then remains stable for at least 50 cycles.

#### 3.3. Structural properties of $\text{Li}_2\text{PtO}_3$

In order to investigate the rechargeable mechanism in the 4 V region, we used XRD to measure the structural changes in the  $\text{Li}_{2-x}\text{PtO}_3$  cathode pellets on charging up to  $x = 1.2$ . Fig. 6 shows the behavior of the (00c) and (a00) peaks of  $\text{Li}_2\text{PtO}_3$  during the initial charging process. The variation in the lattice parameters and unit cell volume were independently calculated from Fig. 6(a) to (b). As  $x$  in  $\text{Li}_{2-x}\text{PtO}_3$  increases from 0 to 1.2, the interlayer spacing decreases slightly and the intralayer distance increases a little as shown in Fig. 7. In addition, some distinct peaks which are probably caused by a lithium depleted phase can be seen at  $2\theta = 18.1^\circ$ ,  $21.3^\circ$ ,  $34.1^\circ$ ,  $41.5^\circ$  and  $47.9^\circ$  for  $x > 0.8$  in  $\text{Li}_{2-x}\text{PtO}_3$  and this phase disappears reversibly

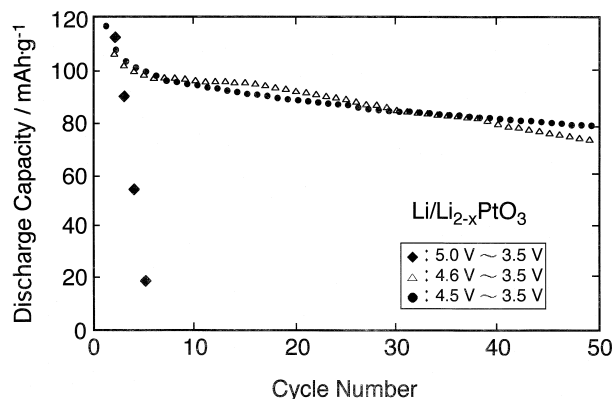


Fig. 5. Cyclability of  $\text{Li}/\text{Li}_2\text{PtO}_3$  cell at a rate of  $0.5 \text{ mA/cm}^2$  in various voltage ranges;  $\bullet$ : between 3.5 and 4.5 V,  $\Delta$ : between 3.5 and 4.6 V, and  $\blacklozenge$ : between 3.5 and 5.0 V.

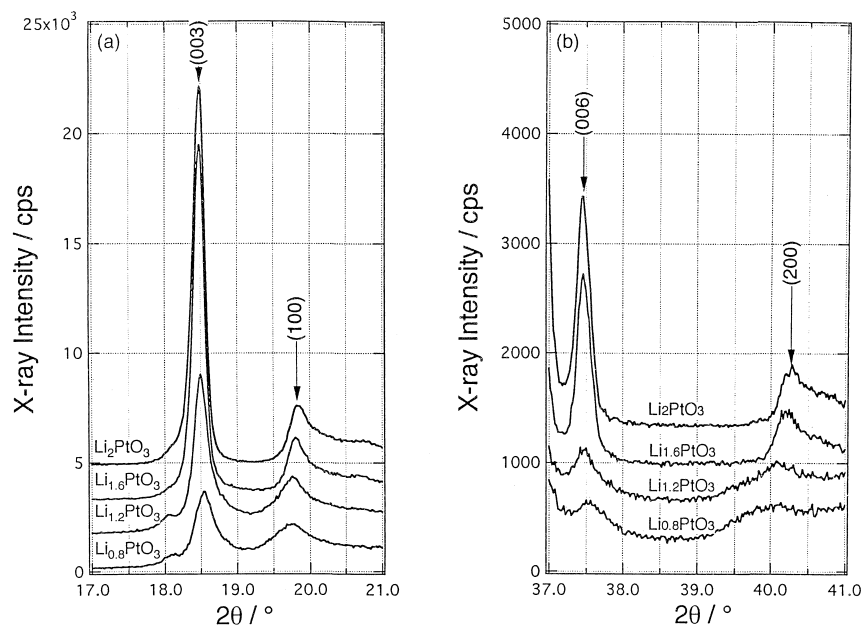


Fig. 6. Behavior of (00c) and (a00) Bragg diffraction peaks of  $\text{Li}_{2-x}\text{PtO}_3$  during charging up to  $x = 1.2$ ; (a) (003) and (100) peaks, (b) (006) and (200) peaks.

on discharge. The interlayer spacing is usually decreased by lithium extraction on charging in layered transition metal dichalcogenides such as  $\text{Li}_{1-x}\text{TiS}_2$ , while it increases on charging in layered rocksalt oxides such as

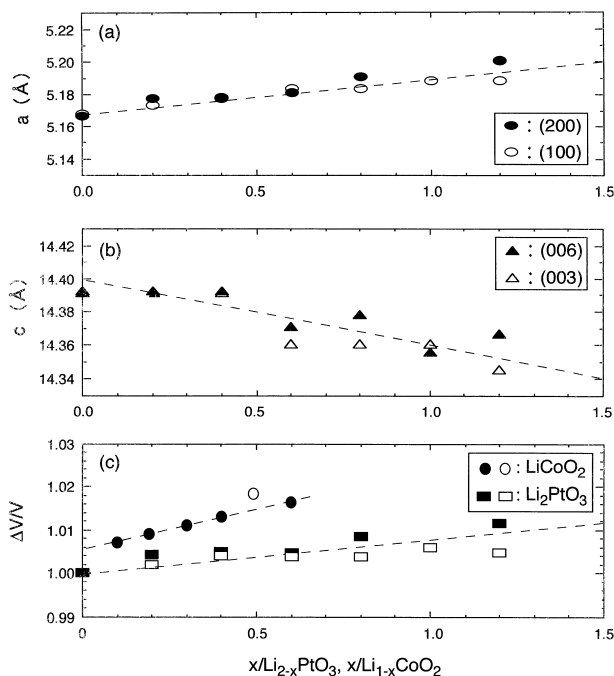


Fig. 7. Variations in unit cell with Li extraction from  $\text{Li}_2\text{PtO}_3$ ; (a)  $a$ -lattice parameter variation: the open and solid ovals were calculated from (100) and (200) peak shifts, respectively, (b)  $c$ -lattice parameter variation: the open and solid triangles were calculated from (003) and (006) peak shifts, respectively, and (c) unit cell volume variation compared to that of  $\text{LiCoO}_2$  [9]: the open and solid circles show hexagonal and monoclinic phases of  $\text{LiCoO}_2$ , respectively.

$\text{Li}_{1-x}\text{CoO}_2$  as a result of the strong ionicity of the M–O bonds. The behavior of the  $\text{Li}_2\text{PtO}_3$  system is intermediate because the Pt–O bonds have a higher covalency than the Co–O bonds in  $\text{LiCoO}_2$ . The relatively mild repulsion between adjacent oxygen layers in  $\text{Li}_{2-x}\text{PtO}_3$  makes the layer structure with an empty van der Waals gap more thermodynamically stable than in  $\text{LiMO}_2$ . This leads to a suppression of the unit cell volume change ratio,  $\Delta V/V$ , to less than 1.5% during the cycling process, as shown in Fig. 7(c) and enlarges the reversible intercalation composition limit, for example  $x < 1$  in  $\text{Li}_{1-x}\text{TiS}_2$  and  $x < 1.2$  in  $\text{Li}_{2-x}\text{PtO}_3$ , while  $x < 0.5$  in  $\text{Li}_{1-x}\text{CoO}_2$ .

The XRD profiles of  $\text{Li}_2\text{PtO}_3$  cathode pellets after 100th cycle are compared with that of the initial pellet in Fig. 8. The broad peaks around  $2\theta = 26^\circ$  in the XRD profile were caused by the Mylar films in which the pellets

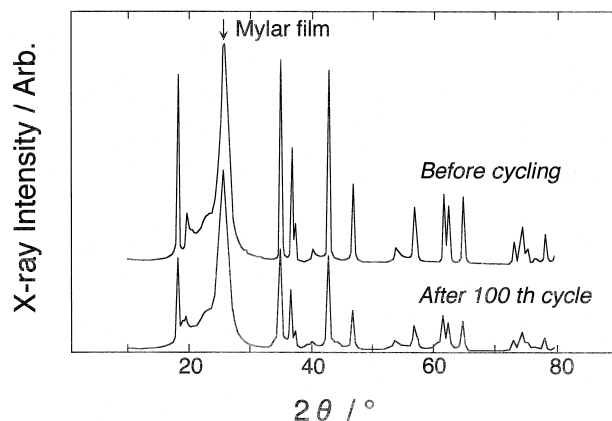


Fig. 8. XRD profiles of  $\text{Li}_2\text{PtO}_3$  cathode pellet; top: before cycling, bottom: after 100th cycle.

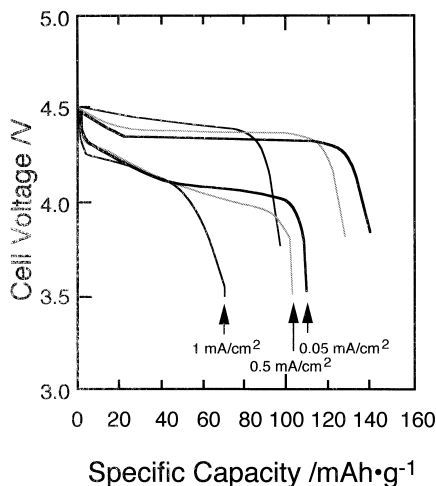


Fig. 9. Rate capability of Li/Li<sub>2-x</sub>PtO<sub>3</sub> cell; thick line: 0.05 mA/cm<sup>2</sup> (1.1 mA/g), dotted line: 0.5 mA/cm<sup>2</sup> (10 mA/g), thin line: 1.0 mA/cm<sup>2</sup> (19 mA/g).

were wrapped to protect them from moisture. The comparison of the two XRD diffraction profiles revealed no significant degradation in any specific peaks. Even after the 100th cycle, Li<sub>2</sub>PtO<sub>3</sub> still retained a basal layered rocksalt structure in the 4 V region, although the crystallinity of the 100th cycle cathode is lost a little.

### 3.4. Kinetic properties of Li<sub>2</sub>PtO<sub>3</sub>

The rate capability of Li<sub>2-x</sub>PtO<sub>3</sub> is shown in Fig. 9. It reveals a relatively small overpotential in the charged state  $x > 0.5$  in Li<sub>2-x</sub>PtO<sub>3</sub>.

## 4. Conclusion

We undertook the electrochemical delithiation of Li<sub>2</sub>PtO<sub>3</sub> in the hope of finding a cathode performance similar to that of layered rocksalt oxide LiCoO<sub>2</sub>. We found that Li<sub>2-x</sub>PtO<sub>3</sub> has a 4 V region vs. Li<sup>0</sup>/Li<sup>+</sup> over a wide composition range of  $x(0.2 < x < 1.2)$ . To date, Li<sub>2-x</sub>PtO<sub>3</sub>

is a unique 4 V cathode with a volumetric capacity comparable to that of LiCoO<sub>2</sub> even among 5d transition metal compounds. Much cathode research has been directed to the first-row 3d transition metal oxides which have high energy densities by weight. Although 5d transition metals are neither light nor inexpensive, this good result with Li<sub>2</sub>PtO<sub>3</sub> encourages us to look for novel cathode materials among the 4d and 5d transition metal oxides. This is because the disadvantages of 4d and 5d transition metal oxide cathodes, their heaviness and expense, should not be critical in terms of applications such as solid state micro-batteries.

## Acknowledgements

The authors would like to express their gratitude to Prof. J. Yamaki of Kyushu University and Dr. I. Yamada of NTT Integrated Information and Energy Systems Laboratories for their encouragement during the course of this research. The authors are also grateful for Dr. H. Ohtsuka's excellent assistance with the kinetic properties measurements.

## References

- [1] K. Mizushima, P.C. Jones, P.J. Wiseman, J.B. Goodenough, *Mater. Res. Bull.* 15 (1980) 783–789.
- [2] J.L. Hodeau, M. Marezio, A. Santoro, R.S. Roth, *J. Solid State Chem.* 45 (1982) 170–179.
- [3] A.C.W.P. James, J.B. Goodenough, *J. Solid State Chem.* 76 (1988) 87–96.
- [4] H. Kobayashi, R. Kanno, Y. Kawamoto, M. Tabuchi, O. Nakamura, M. Takano, *Solid State Ionics* 82 (1995) 25–31.
- [5] H. Kobayashi, R. Kanno, M. Tabuchi, H. Kageyama, O. Nakamura, M. Takano, *J. Power Sources* 68 (1997) 686–691.
- [6] M.H. Rossouw, M.M. Thackeray, *Mater. Res. Bull.* 26 (1991) 463–473.
- [7] K. Asakura, H. Arai, S. Okada, S. Tobishima, J. Yamaki, *Denki Kagaku* 66 (1998) 221–222.
- [8] G.T.K. Fey, W. Li, J.R. Dahn, *J. Electrochem. Soc.* 141 (1994) 2279–2282.
- [9] J.N. Reimers, J.R. Dahn, *J. Electrochem. Soc.* 139 (1992) 2091–2097.